Cyclin A2 modulates kinetochore–microtubule attachment in meiosis II

Qing-Hua Zhang,[1,2] Wai Shan Yuen,[1,2] Deepak Adhikari,[1,2] Jennifer A. Flegg,[3] Greg FitzHarris,[4,5] Marco Conti,[6] Piotr Sicinski,[7,8] Ibtissem Nabti,[9,10] Petros Marangos,[9,11,12] and John Carroll[1,2,9]

[1]Development and Stem Cell Program, Monash Biomedicine Discovery Institute, [2]Department of Anatomy and Developmental Biology, and [3]Monash Academy for Cross and Interdisciplinary Mathematical Applications, Monash University, Melbourne, Victoria, Australia
[4]Centre de Recherche du Centre Hospitalier de l'Université de Montréal, Montréal, Québec, Canada
[5]Department of Obstetrics and Gynaecology, University of Montréal, Montréal, Québec, Canada
[6]Department of Obstetrics, Gynecology, and Reproductive Sciences, Eli and Edythe Broad Center of Regeneration Medicine and Stem Cell Research, Center for Reproductive Sciences, University of California, San Francisco, San Francisco, CA
[7]Dana–Farber Cancer Institute, Boston, MA
[8]Department of Genetics, Harvard Medical School, Boston, MA
[9]Department of Cell and Developmental Biology, University College London, London, England, UK
[10]Division of Science, New York University Abu Dhabi, Abu Dhabi, United Arab Emirates
[11]Department of Biological Applications and Technology, University of Ioannina, Ioannina, Greece
[12]Department of Biomedical Research, Institute of Molecular Biology and Biotechnology–Foundation for Research and Technology, Ioannina, Greece

Cyclin A2 is a crucial mitotic Cdk regulatory partner that coordinates entry into mitosis and is then destroyed in prometaphase within minutes of nuclear envelope breakdown. The role of cyclin A2 in female meiosis and its dynamics during the transition from meiosis I (MI) to meiosis II (MII) remain unclear. We found that cyclin A2 decreases in prometaphase I but recovers after the first meiotic division and persists, uniquely for metaphase, in MII-arrested oocytes. Conditional deletion of cyclin A2 from mouse oocytes has no discernible effect on MI but leads to disrupted MII spindles and increased merotelic attachments. On stimulation of exit from MII, there is a dramatic increase in lagging chromosomes and an inhibition of cytokinesis. These defects are associated with an increase in microtubule stability in MII spindles, suggesting that cyclin A2 mediates the fidelity of MII by maintaining microtubule dynamics during the rapid formation of the MII spindle.

Introduction

Successful progression through meiosis is a crucial process for gamete development. In meiosis I (MI), homologous chromosomes are held together by chiasmata, whereas sister chromatids are coupled by the cohesin complex. The first meiotic division is initiated just before ovulation and is driven by the anaphase-promoting complex/cyclosome (APC/C)–mediated destruction of securin and cyclin B (Brunet and Maro, 2005; Homer et al., 2005; Peters, 2006; Holt and Jones, 2009). The loss of securin releases separase, which cleaves cohesin from chromosome arms, thereby allowing the resolution of chiasmata, separation of homologous chromosomes, and extrusion of the first polar body (Pb1; Nasmyth, 2002; Uhlmann, 2003; Kudo et al., 2006). This is rapidly followed by an increase in cyclin B–Cdk1 activity and formation of the second meiotic spindle, which remains stably arrested at meiosis II (MII) until fertilization breaks the Emi2-mediated inhibition of the APC/C (Marangos and Carroll, 2004; Ajduk et al., 2008). At fertilization (or parthenogenetic activation), an increase in Ca^{2+} leads to the destruction of Emi2, thereby releasing the brake on the APC/C and allowing destruction of securin and cyclin B (Rauh et al., 2005; Madgwick et al., 2006; Shoji et al., 2006). At exit from MII, separase removes cohesin from centromeric regions of sister chromatids, allowing sister separation (anaphase II) and exit from meiosis as marked by the extrusion of the second polar body (Pb2; Rattani et al., 2014).

Much attention has been focused on the role of cyclin B–Cdk1 on progression through both mitotic and meiotic cell divisions. In contrast, the role of cyclin A, the first cyclin ever cloned (Swenson et al., 1986), has received less attention. In higher vertebrates, there are two cyclin A isoforms: cyclin A1 and cyclin A2 (Minshull et al., 1990; Howe et al., 1995; Sweeney et al., 1996; Yang et al., 1997). Cyclin A1 is expressed almost exclusively in testes and is restricted to a role in male germ

Correspondence to John Carroll: j.carroll@monash.edu; Qing-Hua Zhang: qinghua.zhang@monash.edu

Abbreviations used: APC/C, anaphase-promoting complex/cyclosome; GV, germinal vesicle; GVBD, germinal vesicle breakdown; hCG, human chorionic gonadotropin; IBMX, 3-isobutyly-1-methylx-anthine; kMT, kinetochore microtubule; kt–mt, kinetochore–MT; MI, meiosis I; MII, meiosis II; MT, microtubule; PAGFP, photoactivatable GFP.

The Rockefeller University Press
J. Cell Biol. Vol. 216 No. 10 3133–3143
https://doi.org/10.1083/jcb.201607111

cell meiosis (Liu et al., 1998), whereas cyclin A2 is widely expressed, and genetic deletion in mice results in peri-implantation lethality (Murphy et al., 1997). In invertebrates, *Caenorhabditis elegans*, and *Drosophila melanogaster*, there is a single isoform of cyclin A that plays important roles in controlling progression through mitosis (Kreutzer et al., 1995; Sigrist et al., 1995; McCleland et al., 2009).

In mitotic cell cycles, cyclin A2 begins to accumulate in the S phase and continues to increase through the S and G2 phases before peaking in early prometaphase. At this point, within minutes of nuclear envelope breakdown (NEBD), cyclin A2 is destroyed by the APC/C (Girard et al., 1991; Erlandsson et al., 2000; den Elzen and Pines, 2001; Pesin and Orr-Weaver, 2007; Wolthuis et al., 2008). This prometaphase destruction occurs in the face of an active spindle assembly checkpoint (SAC; den Elzen and Pines, 2001; Geley et al., 2001; Wolthuis et al., 2008) and leads to the clearance of cyclin A2 before cells reach the metaphase state (den Elzen and Pines, 2001). The established role for cyclin A2 in progression through the S and G2 phases of the cell cycle (Walker and Maller, 1991; Furuno et al., 1999; Winston et al., 2000; Gong et al., 2007; Kalaszczynska et al., 2009) is consistent with its expression profile during this period. Similarly, inducing persistent expression of cyclin A2 through metaphase leads to disrupted microtubule–kinetochore interactions and delays entry into anaphase (Pines and Hunter, 1990, 1991; den Elzen and Pines, 2001), whereas depleting cyclin A2 leads to a significant increase in the fraction of cells displaying lagging/bridge chromosomes in anaphase (Godek et al., 2015; Kanakkanthara et al., 2016). Thus, cyclin A2 clearly has important roles in mitotic cell cycles, but the embryonic lethality of cyclin A2 knockout mice has restricted investigation into its role in female meiosis (Winston et al., 2000; Persson et al., 2005).

Cyclin A2 is expressed in ovarian and ovulated oocytes at the level of mRNA and protein (Winston et al., 2000; Fuchimoto et al., 2001; Persson et al., 2005; Wolgemuth, 2011; Touati et al., 2012). The functional role of cyclin A2 in meiosis has recently been investigated by injecting mouse oocytes with anti–cyclin A2 antibodies at different stages of meiosis to acutely inhibit cyclin A2 function. The effects include inhibition of the G2–M transition as indicated by delayed germinal vesicle breakdown (GVBD), and in MII oocytes there is a dramatic failure to separate sister chromatids at the time of egg activation (Touati et al., 2012). In this study, we used the ZP3–Cre–LoxP system to specifically delete the cyclin A2 gene from growing oocytes (Fig. S1; Lewandoski et al., 1997; Lan et al., 2004). We report that cyclin A2–deficient oocytes progress through the G2–M transition and MI unhindered; however, nearly 40% of the oocytes show disrupted MII spindles, an increase in merotelic attachments, and a dramatic increase in lagging chromosomes on exit from MII. Our data reveal that cyclin A2 plays an essential role specifically in MII and in the oocyte to embryo transition.

Results

Cyclin A2 is necessary for normal MII spindle formation

Similar numbers of oocytes were ovulated in hormone-primed *cyclin A2*$^{fl/fl}$ and *cyclin A2*$^{-/-}$ females (Fig. 1 a). To test our strategy for deleting cyclin A2 from oocytes, Western blotting was performed on oocytes from *cyclin A2*$^{-/-}$ and *cyclin A2*$^{fl/fl}$ mice as controls. The *Zp3 Cre* was highly effective at reducing cyclin A2 levels to <3% of controls (Fig. S1, c and d).

Having established that cyclin A2 was effectively depleted, we used immunofluorescence and Hoechst labeling to examine the meiotic status of ovulated oocytes. This revealed that 37% of 71 ovulated MII-stage *cyclin A2*$^{-/-}$ oocytes showed errors in MII spindle formation compared with <3% of *cyclin A2*$^{fl/fl}$ oocytes (Fig. 1 b). The abnormalities seen in *cyclin A2*$^{-/-}$ oocytes included multipolar spindles and spindles with chromatin detached from the metaphase plate; some oocytes showed microtubule (MT) asters throughout the cytoplasm (Fig. 1 c). To examine the specificity of these observations, we microinjected cyclin A2 mRNA into germinal vesicle (GV)–stage *cyclin A2*$^{-/-}$ oocytes before in vitro maturation. The expression of cyclin A2 during maturation resulted in an increase in cyclin A2 protein in MII-stage oocytes (Fig. S2 c) and a concomitant decrease in spindle abnormalities (Fig. S2 a). The abnormalities in the MII spindle of *cyclin A2*$^{-/-}$ oocytes suggest that cyclin A2 plays a critical role in the formation of the MII spindle—a process that has received much less attention than formation of the MI spindle.

To examine when the MII spindle abnormalities first appeared, we used 4D live-cell confocal microscopy to image MII spindle formation in oocytes expressing EB1-GFP to visualize MTs and Hoechst 33342 stain to label DNA. Imaging began 8.5–9 h after release from 3-isobutyly-1-methylx-anthine (IBMX; Fig. S3 and Videos 1, 2, and 3), ∼1 h before extrusion of the first polar body, and continued through the interkinesis period, defined herein as the period from polar body formation to arrest at MII. In control oocytes, the interkinesis DNA remained clumped together, and bipolarity of the MII spindle was achieved in all oocytes within 20 min of the first polar body extrusion. Thereafter, the MII spindle increased in length, with chromosomes gradually becoming individualized but never straying from the spindle midzone. In contrast, in all *cyclin A2*$^{-/-}$ oocytes examined, bipolarity was never established within 20 min and instead was achieved 40–60 min after formation of the first polar body. Once bipolarity was established, the chromosomes migrated from the midzone and were distributed over the developing spindle. These observations are consistent with the abnormal spindles identified in ovulated MII oocytes and suggest that the ability to form a bipolar MII spindle and to retain balanced forces on the chromosomes is compromised in the absence of cyclin A2.

Cyclin A2 is not required for MI

We next asked whether the MII spindle phenotypes had their origins in tMI. Comparison of timing of GVBD and polar body formation between *cyclin A2*$^{-/-}$ oocytes and *cyclin A2*$^{fl/fl}$ oocytes revealed no significant difference in timing of GVBD, polar body formation, and entry into MII (Fig. 2, a and b). To closely examine the first meiotic spindle, the origin of the most aneuploidy (Hassold and Hunt, 2001), MI-stage oocytes were fixed and spindle organization was compared. Remarkably, no discernible differences were detected in either the size of the spindles or the alignment of the chromosomes (Fig. 2, c and d). Furthermore, the use of cold treatment and kinetochore and MT labeling to reveal kinetochore-attached MTs (Shomper et al., 2014) revealed that 77% of kinetochore pairs in *cyclin A2*$^{-/-}$ oocytes showed correct polar MT attachment compared with 79.1% of control *cyclin A2*$^{fl/fl}$ oocytes (Fig. 2, e and f). The normality of MI in a cyclin A2–null background was further

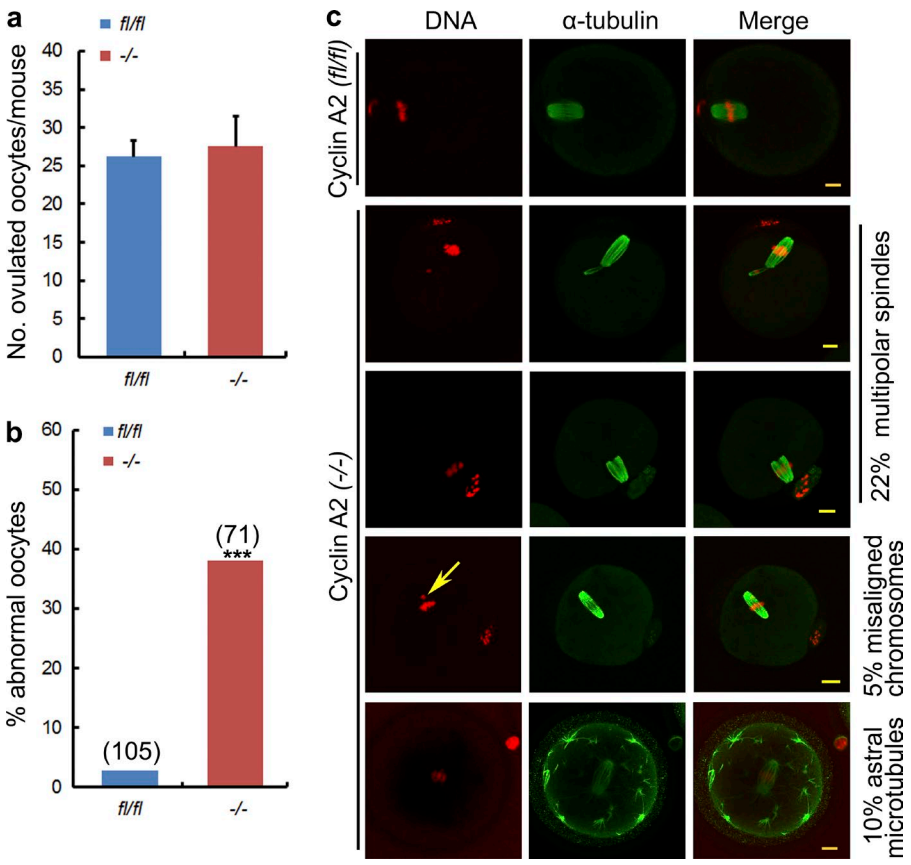

Figure 1. **Ovulated *cyclin A2*$^{-/-}$ oocytes show abnormal MII-stage spindles.** (a) After superovulation, *cyclin A2*$^{-/-}$ and *cyclin A2*$^{fl/fl}$ mice show no significant difference in the number of ovulated oocytes (n = 5 mice for each genotype). Error Bars represent SEM; P > 0.1 by t test. (b) Ovulated oocytes from the *cyclin A2*$^{-/-}$ mice showed higher rates of spindle abnormality (37%, n = 71) than those from the *cyclin A2*$^{fl/fl}$ group (2.9%, n = 105). ***, P < 0.001 by χ^2 test. The number in parentheses is the number of oocytes analyzed. (c) Examples of spindle phenotypes in ovulated oocytes from *cyclin A2*$^{fl/fl}$ mice (top row) and *cyclin A2*$^{-/-}$ mice (all other rows). The percentage of *cyclin A2*$^{-/-}$ oocytes showing each named phenotype is provided. Arrow shows misaligned chromosomes. Bars, 10 µm.

supported by the finding that no aneuploidy was seen in the chromosome spreads of *cyclin A2*$^{-/-}$ MII-stage oocytes (Fig. S4). These findings show that cyclin A2 is dispensable for formation of a functional first meiotic spindle and has no observable impact on the timing or fidelity of meiotic progression in MI.

Cyclin A2 protein levels increase in MII oocytes

The role of cyclin A2 specifically during MII suggests that the dynamics of cyclin A2 expression may be different from those seen in mitosis, where it is destroyed at the prometaphase–metaphase border (Di Fiore and Pines, 2010; Kabeche and Compton, 2013). To examine the expression profile of cyclin A2 during meiosis, oocytes were examined at G2/prophase arrest (GV), in early prometaphase 2 h after release from arrest (GVBD), in metaphase of MI (MI) 8 h after release, and after superovulation (MII). Western blot analysis showed that the cyclin A2 level was stable in early prometaphase and then declined by ∼30% in the MI stage. From MI to MII, the level of cyclin A2 increased approximately threefold and was double that seen in the GV and GVBD stages (Fig. 3, a and b).

To examine the mechanism underpinning the increase in cyclin A2 protein between MI and MII, we examined the amount of polysome-associated cyclin A2 transcript at different stages of meiosis and compared it to that of securin. The data reveal that there is a threefold increase in polysome-associated cyclin A2 mRNA in MII oocytes compared with the GV or MI stages (Fig. 3 c, left). In contrast, polysome-associated securin remains constant throughout all stages (Fig. 3 c, right). Together, these data suggest that cyclin A2 translation is up-regulated late in meiosis, reaching a maximum in MII-stage oocytes—an expression pattern consistent with the observed MII phenotype.

Cyclin A2$^{-/-}$ oocytes have an increased rate of lagging chromosomes during MII exit

The abnormalities in MII spindles observed in the present study and previous observations indicating that inhibition of cyclin A2 prevents sister separation (Touati et al., 2012) strongly suggest that *cyclin A2*$^{-/-}$ oocytes may fail to exit from MII. Therefore, we examined the ability of *cyclin A2*$^{-/-}$ oocytes to undergo the second meiotic division in response to a brief exposure to 7% ethanol, a routine approach to triggering exit from MII. Time-lapse confocal imaging of oocytes undergoing MII exit revealed that similar proportions of control and *cyclin A2*$^{-/-}$ oocytes underwent sister chromatid separation (96.2% vs. 89.4%, respectively) and that the time to initiation of anaphase was similar in *cyclin A2*$^{-/-}$ and control oocytes (17.1 ± 1.5 and 15.6 ± 1.1 min, respectively; Fig. 4 b). Polar body extrusion was reduced in *cyclin A2*$^{-/-}$ oocytes (96.2% and 56.7%, respectively), but even in these oocytes, 31.7% underwent sister separation and were arrested with aberrant anaphase and telophase structures (Fig. 4 a). The most dramatic phenotype was revealed on close examination of anaphase in oocytes that extruded the polar body. The vast majority of *cyclin A2*$^{-/-}$ oocytes (75.4%) showed lagging chromosomes during anaphase compared with controls (16%; Fig. 4 a). Together, these data confirm that cyclin A2 is dispensable for sister separation and instead plays a major role in spindle and chromosome organization during progression into and out of MII.

A high frequency of lateral and merotelic attachments during MII in *cyclin A2*$^{-/-}$ oocytes.

Merotelic attachments are a feature of MII spindle formation (Kouznetsova et al., 2014), and the origin of lagging chromo-

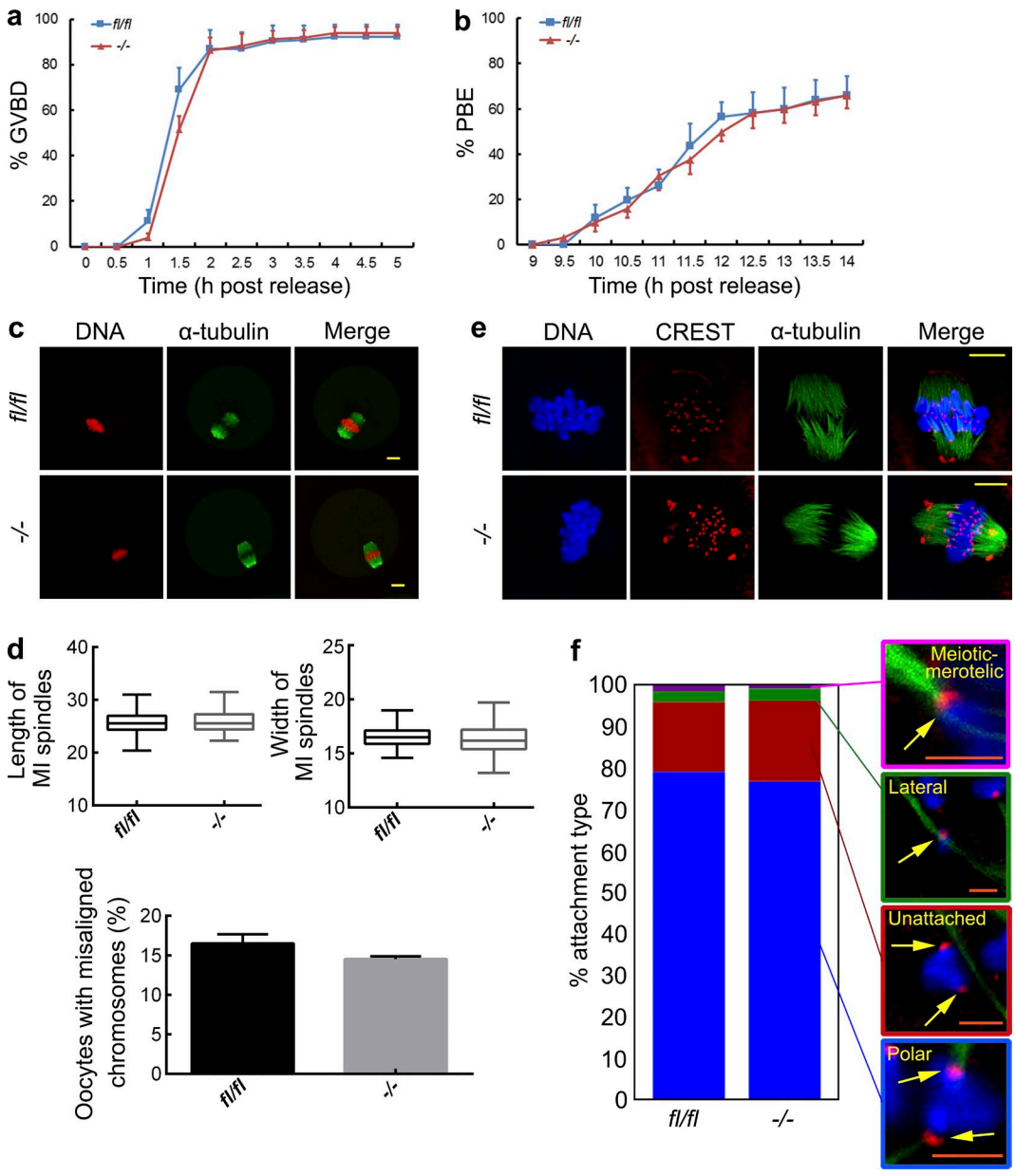

Figure 2. **Cyclin A2 is not necessary for progression through MI.** (a) Rates of GVBD in *cyclin A2*$^{fl/fl}$ (n = 102) and *cyclin A2*$^{-/-}$ (n = 106) groups. P > 0.05, by *t* test. Data is mean and SEM from four replicate experiments. (b) Rates of polar body extrusion (PBE) in *cyclin A2*$^{fl/fl}$ (n = 92) and *cyclin A2*$^{-/-}$ (n = 82) groups at different time points. P > 0.1, by *t* test. Data is mean and SEM from three replicate experiments. (c) MI oocytes from *cyclin A2*$^{fl/fl}$ and *cyclin A2*$^{-/-}$ mice showed apparently normal spindle structures confirmed in d by analysis of spindle length (top left), spindle width (top right), and chromosome alignment (bottom). No differences were detected between *cyclin A2*$^{fl/fl}$ (n = 82) and *cyclin A2*$^{-/-}$ (n = 91) groups. Error bars represent SEM. Bars, 10 µm. P > 0.1, by *t* test. (e) kt–mt attachments in cold-treated MI-stage oocytes from *cyclin A2*$^{fl/fl}$ and *cyclin A2*$^{-/-}$ mice. One example of each attachment type observed in MI-stage oocytes is shown. Bars, 10 µm. (f) Analysis of attachment types in oocytes from *cyclin A2*$^{-/-}$ (1,019 attachments from 27 oocytes) and *cyclin A2*$^{fl/fl}$ (839 attachments from 22 oocytes) mice. Colored surroundings of each box correspond to the colors in the quantification of attachment types in each bar. Arrows indicate the kinetochore pair with the described attachment. Bars, 2 µm. P > 0.1 by χ^2 test.

somes in mitosis is attributed to merotelic attachments (Cimini et al., 2001; Thompson and Compton, 2011).

To investigate the role of cyclin A2 in the formation of kinetochore–microtubule (kt–mt) attachments in the MII spindle, we analyzed the attachment types at 12.5 h (early MII) and 14.5 h (mature MII) in control and *cyclin A2*$^{-/-}$ oocytes (Fig. 5). In control oocytes at 12.5 h, the vast majority of kinetochores (78%) had already formed polar attachments, whereas 11% remained unattached, 7% were merotelic (Fig. 5 a, inset 1), and 4% had lateral connections. This contrasted with *cyclin A2*$^{-/-}$ oocytes, in which only just over 10% of kinetochores had polar attachments, with the vast majority showing lateral connections (79.4%; Fig. 5 a, insets 2, 3, and 4). The remaining kinetochores were largely unattached, with less than 1% being merotelic at this time point. By 14.5 h, most of the control oocytes showed a "mature" spindle phenotype, with nearly all kinetochores showing polar attachments (95%; Fig. 5 c, inset 5) and the remainder showing merotelic or lateral attachments. However, in *cyclin A2*$^{-/-}$ oocytes, the transition to polar attachments was significantly delayed such that only 59.4% of kinetochores showed

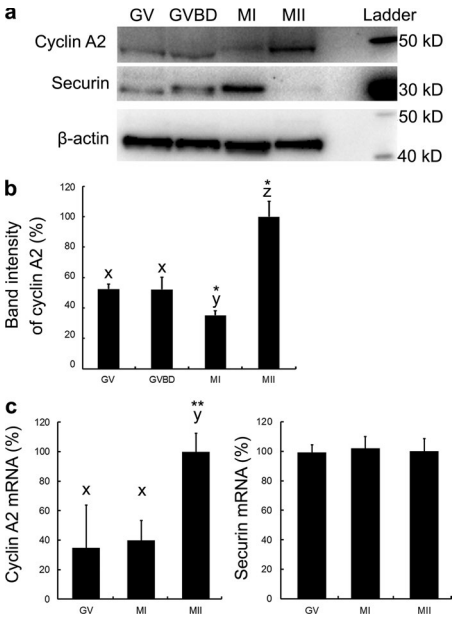

Figure 3. **Expression profile of cyclin A2 in mouse oocytes.** (a) Western blot analysis of cyclin A2 and securin levels in oocytes at different stages of meiosis: GV, GVBD, MI, and MII at 0, 2, and 8 h after release from arrest and superovulated oocytes, respectively (120 oocytes/lane). Data shown in a are representative of three replicate Western blots. Cyclin A2 increases at the MII stage, whereas securin is low. (b) Densitometric analysis of cyclin A2 levels. Data are mean and SEM from three individual experiments analyzed by *t* test. (c) Association of cyclin A2 (left) and securin (right) mRNA to polysomes at the GV, MI, and MII stages. Data are expressed as relative intensities. Data are mean and SEM from three individual experiments by *t* test. *, $P < 0.05$; **, $P < 0.01$.

polar attachments (Fig. 5 d), whereas there was a dramatic increase in merotelic attachments (23.9%; Fig. 5 c, inset 7), and 16.6% of attachments remained lateral (Fig. 5 c, insets 6 and 8). Interestingly, all the chromosomes in the "mini-spindles" seen in the *cyclin A2*$^{-/-}$ oocytes showed lateral attachments (Fig. 5 a, insets 3 and 4; and Fig. 5 c, inset 8). Cyclin A2 therefore plays a critical role in the transition of an "immature" MII spindle, in which the majority of attachments are lateral, to a "mature" spindle with polar kt–mt attachments.

Kinetochore microtubules (kMTs) have a longer half-life in *cyclin A2*$^{-/-}$ oocytes

MT dynamics are critical for error correction and the resolution of merotelic attachments (Thompson and Compton, 2011). Remarkably, cyclin A2 has recently been shown to promote MT turnover in bipolar prometaphase spindles, thereby allowing kt–mt attachment error correction until just before metaphase (Kabeche and Compton, 2013). To examine whether MT stability in *cyclin A2*$^{-/-}$ oocytes may contribute to abnormal kt–mt attachments and lagging chromosomes, we adapted an assay for measuring MT stability for use in MII oocytes (FitzHarris, 2009). To measure MT stability, oocytes were injected with mRNA-encoding photoactivatable GFP (PAGFP)–α-tubulin and matured to the MII stage. The spindle was located using a small amount of coinjected X-rhodamine–labeled tubulin protein, and a line of PAGFP-α-tubulin was photoactivated close to the MII chromosomes by brief illumination with the 405-nm laser (Fig. 6 a). The decay of the PAGFP fluorescence provides a measure of MT stability (Zhai et al., 1995). In mitotic cells, this decay in MTs comprises two components with distinct half-lives: (a) a rapid turnover (short half-life) in the population of non-kMTs and (b) a more stable (longer half-life) component reflecting the kMTs (Zhai et al., 1995; Kabeche and Compton, 2013; Fig. 6). Similarly, we found that the fluorescence decay of the PAGFP in both *cyclin A2*$^{fl/fl}$ and *cyclin A2*$^{-/-}$ oocytes fits a double exponential curve (Fig. 6 b). We found that treatment of oocytes with Taxol stabilizes both populations of MTs, confirming that this assay can measure changes in MT stability (Fig. 6). The half-life of non-kMTs is in the vicinity of 20–30 s, whereas that of kMTs is 2.5 ± 0.5 min in *cyclin A2*$^{fl/fl}$ oocytes and 3.9 ± 0.5 min in *cyclin A2*$^{-/-}$ oocytes (Fig. 6 c). This 56% increase in MT stability strongly supports the idea that at least some of the effects of cyclin A2 on erroneous attachments are mediated via MT stability during MII spindle formation.

Discussion

We used a genetic model to delete cyclin A2 from growing oocytes. Uniquely for metaphase in any cell type thus far studied, mammalian oocytes stabilize cyclin A2 during metaphase II, where it plays a critical role in spindle formation and in the prevention of merotelic attachments and lagging chromosomes during anaphase.

In all cells studied to date, cyclin A2 is destroyed in prometaphase so that its levels are greatly reduced during metaphase. In oocytes, we confirmed that cyclin A2 is destroyed during prometaphase I and remains low during progression through MI, but we were surprised to find that cyclin A2 was present in MII oocytes at levels significantly higher than those seen in prophase-arrested, GV-stage oocytes. The increase in cyclin A2 in MII oocytes appears to be a result of persistent translation as suggested by association with polysomes. Its accumulation may be further enhanced by inhibition of the APC/C by Emi2 during prometaphase II, a pathway that ensures that cyclin B levels can increase rapidly, thereby driving entry into MII (Suzuki et al., 2010; Sako et al., 2014). The presence of cyclin A2 during MII may therefore, in part, be a by-product of the mechanisms invoked to maintain a stable MII arrest as the oocyte awaits fertilization.

The prometaphase destruction of cyclin A2 in mitosis is thought to be important because persistent high levels of cyclin A2 can cause continuous chromosome movements and a delay in entry into anaphase (den Elzen and Pines, 2001), presumably because of its role in destabilizing kt–mt interactions (Kabeche and Compton, 2013; Godek et al., 2015). It is not clear why the MII spindle tolerates cyclin A2 during metaphase and mitotic spindles do not, but the acentriolar nature of meiotic spindles is one obvious difference. More importantly, MT stability and spindle function are directly regulated by high levels of MAPK and the presence of Emi2 during MII, which may be sufficient to allow spindle stabilization in the presence of cyclin A2 (Lefebvre et al., 2002; Terret et al., 2003; Perry and Verlhac, 2008).

Remarkably, cyclin A2 is not only compatible with MII, but it has also acquired critical roles in spindle formation and is necessary to avoid merotelic attachments and lagging chromosomes during MII exit. The split spindle poles (multipolar)—microspindles with isolated chromosomes emanating from the main spindle—the presence of interspindle pole MTs, and some oocytes showing extensive cytoplasmic asters are consistent with a role for cyclin A2 in MT function during progression into MII. Live-cell imaging confirmed that it was during the

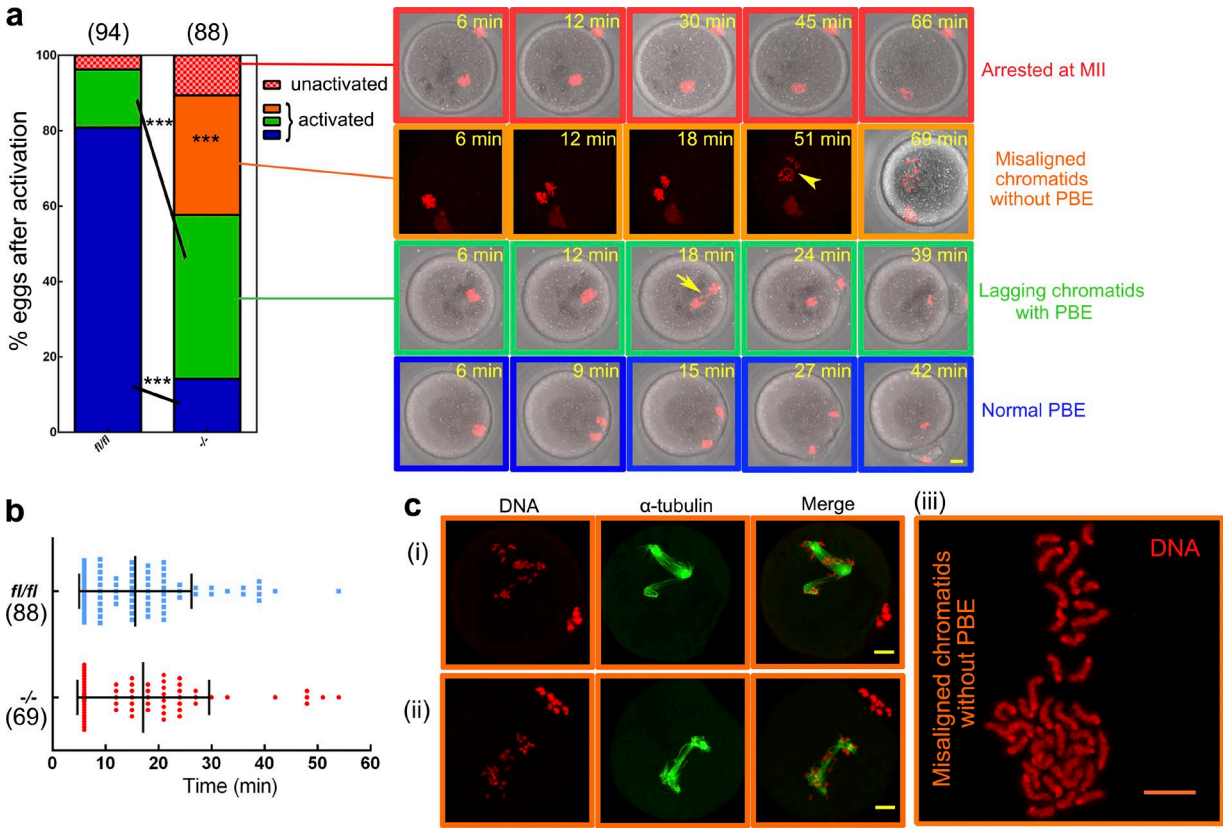

Figure 4. **Cyclin A2 is not required for sister separation at anaphase II but is necessary to avoid lagging chromosomes.** (a) Analysis of anaphase II in *cyclin A2*$^{-/-}$ oocytes. *Cyclin A2*$^{-/-}$ (n = 88) and control (n = 94) oocytes showed similar rates of sister separation (blue + green + orange bars), but the proportion of oocytes undergoing polar body extrusion (PBE) extrusion (blue + green bars) was reduced (57.7% vs. 96.3%, respectively). Lagging chromosomes were significantly increased in *cyclin A2*$^{-/-}$ oocytes compared with *cyclin A2*$^{fl/fl}$ controls (75.4% vs. 16%, respectively). Color coding matches quantification with phenotype as determined by imaging. The numbers in parentheses represent oocyte numbers. Time stamps on images represent time elapsed after transfer to activation stimulus (7% ethanol). Arrows show lagging chromatids. Bar, 10 µm. ***, P < 0.001 by χ^2 test. (b) Time from ethanol exposure to anaphase onset is similar in *cyclin A2*$^{fl/fl}$ (n = 88) and *cyclin A2*$^{-/-}$ (n = 69) oocytes. Error bars represent SEM. P > 0.05 by t test. (c, i and ii) Oocytes that failed to undergo PBE (orange bar) showed highly disrupted MT structures and dispersed individual chromatids. (c, iii) Chromosome spread of *cyclin A2*$^{-/-}$ oocyte that failed to extrude the second polar body. The sister chromatids have undergone separation. Bars: (c, i and ii) 10 µm; (c, iii) 2 µm.

interkinesis period during MII spindle formation (analogous to prometaphase) that loss of cyclin A2 first manifested in spindle defects, including a loss of spindle organization and dispersal of chromosomes over the developing spindle. Closer examination of kt–mt interactions during this period shows that between early metaphase II (12.5 h after human chorionic gonadotropin [hCG]) and "mature" metaphase II (14.5 h), there is a dramatic transition from lateral to polar kt–mt attachments, and this process is disrupted in the absence of cyclin A2. The resultant increase in merotelic and lateral attachments in *cyclin A2*$^{-/-}$ has dramatic consequences for MII exit, leading to a three- to four-fold increase in lagging chromosomes.

The underlying explanation for these defects in spindle and kt–mt interactions is unclear, but the recent finding that cyclin A2 destruction is necessary for switching from unstable to stable kt–mt attachments at the prometaphase–metaphase transition in mitosis is a likely contributing factor (Kabeche and Compton, 2013). In this system, knockdown of cyclin A2 causes premature kt–mt stability in prometaphase and an increase in lagging chromosomes on metaphase exit, similar to the phenotype observed in oocytes. We found in MII spindles of *cyclin A2*$^{-/-}$ oocytes that there is an increase in kt–mt stability that may explain the problems seen in the transition from lateral to polar attachments and the associated failure to correct merotelic attachments.

The demonstrated role of cyclin A2 in MII contrasts dramatically with the failure to detect any impact of cyclin A2 ablation on MI. The timing of the G2–M transition and completion of MI is unaffected in cyclin A2–deficient oocytes, as are the size and shape of the MI spindle, the chromosome alignment, the frequency of kt–mt attachments, and the frequency of aneuploidy. How can this disparity between the roles of cyclin A2 in MI and MII be explained? It may be that MI has additional or more effective approaches to maintaining Aurora kinase–mediated kt–mt instability during prometaphase I, as indicated by the reduced level of phosphorylation seen on Aurora substrates in MII compared with MI (Yoshida et al., 2015). Additionally, it may simply be that the protracted nature of prometaphase I, which lasts ∼7 h compared with ∼1 h in prometaphase II, allows sufficient time to build a spindle and correct any errors of kt–mt attachment.

Although anaphase II in *cyclin A2*$^{-/-}$ oocytes has a high frequency of lagging chromosomes, the ability of the oocytes to undergo sister separation is unhindered. This is to be expected because merotelic attachments are not detected by the SAC (Sluder et al., 1997; Cimini et al., 2001; Gui and Homer, 2012), and we could find no evidence of kinetochore-associated Mad2 in *cyclin A2*$^{-/-}$ oocytes (unpublished data). Inhibition of cyclin A2 using injection of antibodies has

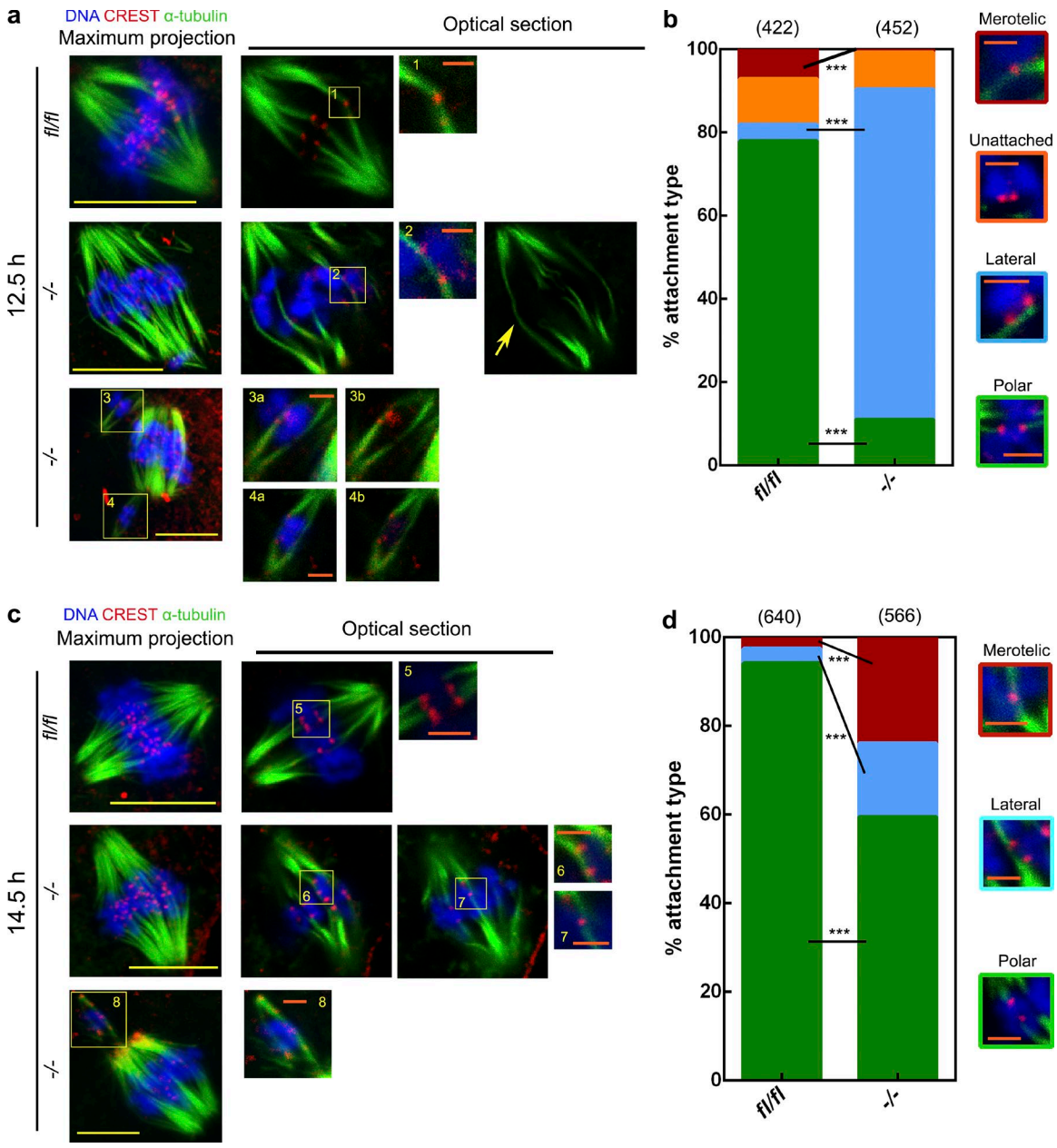

Figure 5. **Cyclin A2 is necessary to prevent a high rate of abnormal kt–mt interactions in MII-stage oocytes.** Representative images of kt–mt attachments in cold-treated control and cyclin A2 knockout oocytes fixed at 12.5 h after hCG as oocytes reach MII (a) and at 14.5 h after hCG when oocytes have arrested at the mature MII stage. Arrow shows stabilized non-kMT. (c). (a and c, insets) Examples of different attachment types (5 shows normal polar attachment; 2 and 6 show lateral attachments; 3, 4, and 8 show examples of attachments in nonspindle chromosomes and microspindles; and 1 and 7 show merotelic attachments). Bars: (yellow) 10 µm; (orange) 2 µm. Analysis of the different attachment types at 12.5 h (b) and 14.5 h (d) in *cyclin A2*$^{fl/fl}$ oocytes (n = 11 and 19, respectively) and *cyclin A2*$^{-/-}$ oocytes (n = 14 and 16, respectively). Numbers in parentheses represent total number of attachments examined. Note the increase in lateral and merotelic attachments and the delay in establishing polar attachments in *cyclin A2*$^{-/-}$ oocytes. ***, $P < 0.001$. Data on attachment types were pooled from the indicated number of oocytes and analyzed using a χ^2 test.

previously indicated a role for cyclin A2 in progression into MI and in sister separation at MII (Touati et al., 2012), neither of which are consistent with the genetic model reported herein. The difference in approach is likely to explain the inconsistency between the two studies. Off-target effects of the antibodies may partly be to blame, but the acute inhibition afforded by antibody injection in wild-type MII oocytes may generate a different phenotype from that seen when oocytes develop in the absence of cyclin A2. In zebrafish and mice (Daude et al., 2012; Banerjee et al., 2013; Smart and Riley, 2013; Kok et al., 2015; Rossi et al., 2015; Wakayama et al., 2015), genetic ablation/mutation can lead to a different phenotype than when the protein is removed acutely via inhibition of translation (morpholinos). At least for some genes, it has been demonstrated that compensation occurs in the case of deleterious mutations but not in the case of more acute, morpholino-based gene knockdowns (Gopinathan et al., 2014). Cyclin E has been shown to compensate for cyclin A in fibroblasts (Winston et al., 2000), but such compensation does not occur in embryonic stem cells, and we found no evidence of cyclin E up-regulation in *cyclin*

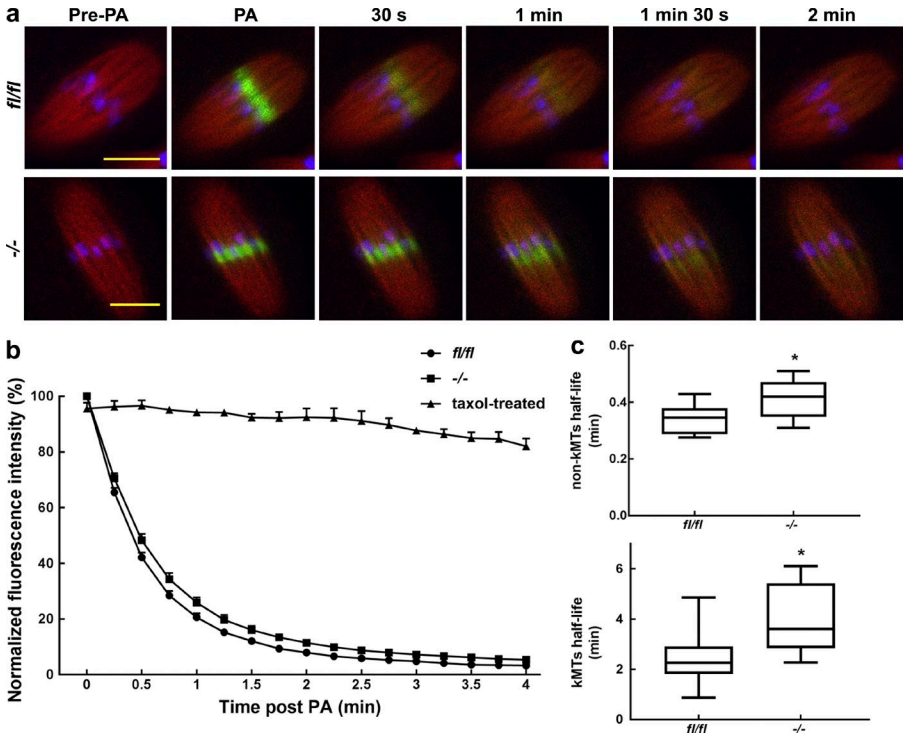

Figure 6. **MT dynamics are altered in cyclin A2 knockout oocytes.** (a) Representative time-lapse images of MII-stage *cyclin A2*$^{fl/fl}$ and *cyclin A2*$^{-/-}$ oocytes. PAGFP-α-tubulin (green) was photoactivated (PA) using a 405-nm laser, and the time course of PAGFP fluorescence decay was monitored. Spindle MTs were visualized using X-rhodamine (red), and chromosomes were visualized using Hoechst 33342 (blue). Bars, 2 µm. (b) Normalized fluorescence decay curves obtained by measuring the loss of PAGFP fluorescence in *cyclin A2*$^{fl/fl}$ ($n = 7$) and *cyclin A2*$^{-/-}$ oocytes ($n = 8$). Decay plots show fast and slow components assumed to represent non-kMTs and kMTs, respectively. Fluorescence decay after Taxol treatment is used to determine the bleaching coefficient for each time point. Error bars represent SEM. (c) Calculated half-life of fast (non-kMTs) and slow (kMTs) shows that MTs have a longer half-life in *cyclin A2*$^{-/-}$ oocytes. Error bars represent SEM. *, $P < 0.05$ by *t* test.

A2$^{-/-}$ oocytes (unpublished data). The genetic approach adopted in this study revealed increases in merotelic attachments and lagging chromosomes in MII oocytes, but we could find no evidence to support a role for cyclin A2 in deprotection of cohesin and subsequent sister separation.

In conclusion, cyclin A2 plays an essential role in ensuring the faithful separation of chromosomes specifically during MII. The absence of an effect in MI defines a clear difference in the role and regulation of kt–mt attachments and error correction between the two meiotic divisions. Whereas in somatic cells, cyclin A2 destruction marks the switch from prometaphase to metaphase, no such switch occurs in MII oocytes, where inhibition of the APC/C for MII arrest also allows the accumulation of cyclin A2. The persistence of cyclin A2 during the prefertilization MII arrest may provide the oocyte with the flexibility in kt–mt attachments for improved error correction during the prolonged MII arrest. Finally, this role of cyclin A2 in ensuring the fidelity of MII has implications for the origins of infertility, where chromosome anomalies in MII are known to contribute to aneuploidy in early mammalian embryos (Hassold and Hunt, 2001).

Materials and methods

Mouse strains and genotyping

Homozygous *cyclin A2*$^{fl/fl}$ mice (C57BL/6J) were obtained from the laboratory of P. Sicinski and crossed with *Zp3-Cre* transgenic mice (C57BL/6J; provided by E. McLaughlin, University of Newcastle, New South Wales, Australia) that specifically express *Cre* in growing oocytes to generate *cyclin A2*$^{-/-}$ oocytes. Control animals were littermates possessing two *loxP*-flanked alleles without *Cre* (*cyclin A2*$^{fl/fl}$), as shown in Fig. S1 a. Genotyping of cyclin A2 knockout mice was performed as described previously (Kalaszczynska et al., 2009) with primers p1 (5′-CGCAGCAGAAGCTCAAGACTCGAC-3′) and p2 (5′-TCTACATCCTAATGCAATGCCTGG-3′; Fig. S1 b).

Oocyte culture and manipulation

Oocytes were collected from 4–6-wk-old female mice. For in vitro maturation, GV oocytes were collected in M2 medium (Sigma-Aldrich) containing 200 µM IBMX. Culture was performed in drops of M16 medium (Sigma-Aldrich) under mineral oil (Sigma-Aldrich) at 37°C in a humidified atmosphere of 5% CO_2 in air. For cold treatment, oocytes were incubated in 4°C M2 medium for 10 min (MI stage) or 8 min (MII stage). For collection of MII-stage oocytes, mice were superovulated by sequential intraperitoneal injections of 8 IU pregnant mare's serum gonadotropin (PMSG; Intervet) and 8 IU human chorionic gonadotropin (hCG; Intervet) at an interval of 48 h before culling the mice and collecting the eggs from oviducts. Parthenogenesis was performed using 7% ethanol for 5 min at 37°C at 16–18 h after hCG or after 18 h of in vitro culture from the GV stage. MII-stage oocytes from *cyclin A2*$^{fl/fl}$ and *cyclin A2*$^{-/-}$ mice were collected and exposed to ethanol to induce parthenogenetic activation. For collection of one-cell zygotes, mice were placed with a male immediately after hCG, and fertilized eggs were released from the oviduct after 24 h.

In vitro transcription and microinjections

Cyclin A2–GFP mRNA (a gift from J. Pines, The Institute of Cancer Research, London, England, UK) was transcribed using the T7 mMessage mMachine kit (Ambion) according to the manufacturer's protocol and resuspended in RNase-free water. mRNA (1.2 mg/ml) was delivered using a microinjection apparatus consisting of Narishige micromanipulators mounted on a Zeiss S100TV inverted microscope. A controlled delivery of ∼5% oocyte volume was delivered to GV stage–arrested oocytes using a picopump. After injection, oocytes were washed out of IBMX and transferred in M16 medium. For Western blot, the injected GV oocytes were arrested for 2 h (imitating the time from GV to GVBD) in 200 µM IBMX for the expression of mRNA before collection.

Western blot

Oocytes were collected in SDS sample buffer and heated for 10 min at 70°C. Proteins were fractionated at 200 V for 50 min using a 10% NuPAGE Bis-Tris precast gel (Invitrogen) and MOPS running buffer.

Proteins were blotted onto polyvinylidene fluoride membranes for 1.5 h at 30 V, and then the membrane was blocked in TBST containing 5% skimmed milk for 2 h, followed by incubation overnight at 4°C with mouse monoclonal anti–cyclin A antibody (1:500; c4710; Sigma-Aldrich). Mouse anti-securin (1:500; ab3305; Abcam) and mouse anti–β-actin (1:1,000; ab3280; Abcam) antibodies were also used for Western blot. For primary antibody detection, we used a goat HRP–conjugated anti–mouse secondary antibody (1:1,000; 1 h at 37°C; P0447; Dako). Finally, the membrane was processed using standard ECL techniques (GE Healthcare) and processed using the ChemiDoc MP imaging system (Bio-Rad). Densitometric analyses of band intensities were performed with ImageJ software.

Immunofluorescence and imaging

Oocytes or eggs were fixed in a solution of 4% paraformaldehyde and 2% Triton X-100 in PBS for 40 min at 25°C. Blocking was performed in PBS with 10% BSA and 2% Tween for 60 min at 25°C. The following antibodies were used for immunolabeling: CREST (1:50; 90C-CS1058; Fitzgerald) and FITC-conjugated mouse anti–α-tubulin (1:200; Alexa Fluor 488; Invitrogen). Goat anti–human IgG antibody (1:100; Alexa Fluor 555; Invitrogen) was used to detect CREST. For analysis of cold-stable MTs, MI-stage oocytes were exposed to ice-cold M2 media for 10 min immediately before fixation, and MII-stage oocytes were exposed to ice-cold M2 media for 8 min immediately before fixation. DNA was labeled using 10-min incubation in Hoechst 33342 (10 µg/ml; Sigma-Aldrich). Serial Z sections of fixed oocytes/eggs in 1% PBS were acquired at room temperature in a glass-bottomed dish using a laser-scanning confocal microscope imaging system (SP8; Leica). Imaging of fixed samples was performed using a 63× oil immersion objective (1.4 NA) at 25°C. For live-cell imaging, eggs were microinjected with or without EB1-GFP mRNA and incubated in drops of M2 medium containing Hoechst 33342 (5 µg/ml) under mineral oil. Live-cell imaging was performed using a Leica SP8 confocal microscope with a 40× water immersion objective (1.1 NA) at 37°C. Image acquisition was performed using Las X software (Leica). Imaris software was used to orient 3D confocal stacks for measurement of spindle length and width.

Photoactivated fluorescence imaging and analysis

PAGFP-α-tubulin mRNA (a gift from G. FitzHarris [University of Montreal, Montreal, Quebec, Canada] and S. Nakagawa [Centre Hospitalier de l'Université de Montréal, Montreal, Canada]) was transcribed using the T7 mMessage mMachine kit according to the manufacturer's protocol and resuspended in RNase-free water. X-rhodamine–labeled tubulin protein (Cytoskeleton, Inc.) was dissolved in general tubulin buffer (Cytoskeleton, Inc.) containing 1 mM GTP sodium salt (Cytoskeleton, Inc.). The final concentration for microinjection was 70 µg/ml. PAGFP-α-tubulin mRNA and X-rhodamine–labeled tubulin were co-injected as described previously. Photoactivation was performed by using the FRAP function on a Leica SP8 confocal microscope with a 40× water immersion objective (1.1 NA) at 37°C. Throughout the experiment, oocytes were in M2 medium containing Hoechst 33342 (5 µg/ml) under mineral oil. Fluorescence decay curves and data analysis were performed as described previously (Kabeche and Compton, 2013). Specifically, for each egg, the decay in PAGFP fluorescence intensity was plotted against time and fitted to a double exponential curve $f(t) = A \times \exp(-k_1 t) + B \times \exp(-k_2 t)$ using MATLAB's cftool, where t represents time; A is the less stable non-kMT population; and B is the kMT population with decay rates of k_1 and k_2, respectively. The half-life for each process was calculated as $\ln 2/k$. Data for which $A > 95\%$ (two oocytes) or where $Re^2 < 0.99$ (one oocyte) were not included in the analysis.

Chromosome spreads

Oocytes were exposed to Acid Tyrodes solution (Sigma-Aldrich) for 1 min at 25°C to remove the zona pellucida. After a 2-min recovery in M2 medium, the oocytes were transferred onto a clean microscope slide that had been previously dipped in a solution of 1% paraformaldehyde in distilled H_2O, pH 9.2, containing 0.15% Triton X-100 and 3 mM dithiothreitol (Hodges and Hunt, 2002). The slides were allowed to dry slowly in a humid chamber overnight, and the fixed oocytes were blocked with 10% BSA and 2% Tween for 1 h at 25°C. The oocytes were then incubated with anti–Bub3 antibody (1:50; H-100; Santa Cruz Biotechnology) overnight at 4°C before being incubated with the goat anti–rabbit IgG antibody (1:100, Alexa Fluor 488) for 2 h at 25°C. DNA on the slides was stained with Hoechst 33342 (10 µg/ml) for 10 min, and slides were mounted for observation using a laser-scanning confocal microscope imaging system as described previously.

Polysome array

Data were obtained from GEO under accession no. GSE35106 (Chen et al., 2011).

Statistical analysis

Data analysis was performed using a *t* test or a χ^2 test with Microsoft Excel and GraphPad Prism Software. Analysis was performed for at least three replicate experiments and is represented as means and SEMs unless otherwise stated. Differences at $P < 0.05$ were considered significant. Level of significance is denoted by *, $P < 0.05$; **, $P < 0.01$; ***, $P < 0.001$. Columns with different letters are significantly differences.

Online supplemental material

Fig. S1 shows the generation of mice with disruption of cyclin A2 in oocytes and the deletion of cyclin A2 in oocytes. Fig. S2 shows that the exogenous expression of cyclin A2 rescues the egg activation phenotype. Fig. S3 shows MII spindle formation in *cyclin A2$^{fl/fl}$* and *cyclin A2$^{-/-}$* oocytes using live-cell imaging. Fig. S4 shows no increase in aneuploidy in *cyclin A2$^{-/-}$* oocytes. Videos show anaphase I to MII transition of *cyclin A2$^{fl/fl}$* (Video 1) and *cyclin A2$^{-/-}$* (Videos 2 and 3) oocytes.

Acknowledgments

We thank Hayden Homer for discussions on the manuscript, Shoma Nakagawa for providing the PAGFP-α-tubulin construct, Duane Compton and Lilian Kabeche for advice on analysis of PAGFP data, Jonathon Pines for providing the cyclin A2–GFP construct, and Eileen McLaughlin for providing the *Zp3-Cre* mice.

This work was supported by a Medical Research Council program grant and an Australian Research Council discovery project grant awarded to J. Carroll and National Institutes of Health grant R01 CA132740-08 awarded to P. Sicinski.

The authors declare no competing financial interests.

Author contributions: Most of the experiments were performed by Q.-H. Zhang. W.S. Yuen, D. Adhikari, G. FitzHarris, I Nabti, and P. Marangos provided support and discussions throughout; J. Flegg analyzed the photoactivation data; M. Conti performed the experiments in Fig. 3 c; and P. Sicinski provided the floxed cyclin A2 mice and contributed to the interpretation of data. J. Carroll coordinated the project and wrote the paper with Q.-H. Zhang.

Submitted: 26 July 2016
Revised: 4 July 2017
Accepted: 28 July 2017

References

Ajduk, A., M.A. Ciemerych, V. Nixon, K. Swann, and M. Maleszewski. 2008. Fertilization differently affects the levels of cyclin B1 and M-phase promoting factor activity in maturing and metaphase II mouse oocytes. *Reproduction.* 136:741–752. http://dx.doi.org/10.1530/REP-08-0271

Banerjee, I., T. Moore Morris, S.M. Evans, and J. Chen. 2013. Thymosin β4 is not required for embryonic viability or vascular development. *Circ. Res.* 112:e25–e28. http://dx.doi.org/10.1161/CIRCRESAHA.111.300197

Brunet, S., and B. Maro. 2005. Cytoskeleton and cell cycle control during meiotic maturation of the mouse oocyte: Integrating time and space. *Reproduction.* 130:801–811. http://dx.doi.org/10.1530/rep.1.00364

Chen, J., C. Melton, N. Suh, J.S. Oh, K. Horner, F. Xie, C. Sette, R. Blelloch, and M. Conti. 2011. Genome-wide analysis of translation reveals a critical role for deleted in azoospermia-like (*Dazl*) at the oocyte-to-zygote transition. *Genes Dev.* 25:755–766. http://dx.doi.org/10.1101/gad.2028911

Cimini, D., B. Howell, P. Maddox, A. Khodjakov, F. Degrassi, and E.D. Salmon. 2001. Merotelic kinetochore orientation is a major mechanism of aneuploidy in mitotic mammalian tissue cells. *J. Cell Biol.* 153:517–528. http://dx.doi.org/10.1083/jcb.153.3.517

Daude, N., S. Wohlgemuth, R. Brown, R. Pitstick, H. Gapeshina, J. Yang, G.A. Carlson, and D. Westaway. 2012. Knockout of the prion protein (PrP)-like *Sprn* gene does not produce embryonic lethality in combination with PrP^{C}-deficiency. *Proc. Natl. Acad. Sci. USA.* 109:9035–9040. http://dx.doi.org/10.1073/pnas.1202130109

den Elzen, N., and J. Pines. 2001. Cyclin A is destroyed in prometaphase and can delay chromosome alignment and anaphase. *J. Cell Biol.* 153:121–136. http://dx.doi.org/10.1083/jcb.153.1.121

Di Fiore, B., and J. Pines. 2010. How cyclin A destruction escapes the spindle assembly checkpoint. *J. Cell Biol.* 190:501–509. http://dx.doi.org/10.1083/jcb.201001083

Erlandsson, F., C. Linnman, S. Ekholm, E. Bengtsson, and A. Zetterberg. 2000. A detailed analysis of cyclin A accumulation at the G_1/S border in normal and transformed cells. *Exp. Cell Res.* 259:86–95. http://dx.doi.org/10.1006/excr.2000.4889

FitzHarris, G. 2009. A shift from kinesin 5-dependent metaphase spindle function during preimplantation development in mouse. *Development.* 136:2111–2119. http://dx.doi.org/10.1242/dev.035089

Fuchimoto, D., A. Mizukoshi, R.M. Schultz, S. Sakai, and F. Aoki. 2001. Posttranscriptional regulation of cyclin A1 and cyclin A2 during mouse oocyte meiotic maturation and preimplantation development. *Biol. Reprod.* 65:986–993. http://dx.doi.org/10.1095/biolreprod65.4.986

Furuno, N., N. den Elzen, and J. Pines. 1999. Human cyclin A is required for mitosis until mid prophase. *J. Cell Biol.* 147:295–306. http://dx.doi.org/10.1083/jcb.147.2.295

Geley, S., E. Kramer, C. Gieffers, J. Gannon, J.M. Peters, and T. Hunt. 2001. Anaphase-promoting complex/cyclosome–dependent proteolysis of human cyclin A starts at the beginning of mitosis and is not subject to the spindle assembly checkpoint. *J. Cell Biol.* 153:137–148. http://dx.doi.org/10.1083/jcb.153.1.137

Girard, F., U. Strausfeld, A. Fernandez, and N.J. Lamb. 1991. Cyclin A is required for the onset of DNA replication in mammalian fibroblasts. *Cell.* 67:1169–1179. http://dx.doi.org/10.1016/0092-8674(91)90293-8

Godek, K.M., L. Kabeche, and D.A. Compton. 2015. Regulation of kinetochore–microtubule attachments through homeostatic control during mitosis. *Nat. Rev. Mol. Cell Biol.* 16:57–64. http://dx.doi.org/10.1038/nrm3916

Gong, D., J.R. Pomerening, J.W. Myers, C. Gustavsson, J.T. Jones, A.T. Hahn, T. Meyer, and J.E. Ferrell Jr. 2007. Cyclin A2 regulates nuclear-envelope breakdown and the nuclear accumulation of cyclin B1. *Curr. Biol.* 17:85–91. http://dx.doi.org/10.1016/j.cub.2006.11.066

Gopinathan, L., S.L. Tan, V.C. Padmakumar, V. Coppola, L. Tessarollo, and P. Kaldis. 2014. Loss of Cdk2 and cyclin A2 impairs cell proliferation and tumorigenesis. *Cancer Res.* 74:3870–3879. http://dx.doi.org/10.1158/0008-5472.CAN-13-3440

Gui, L., and H. Homer. 2012. Spindle assembly checkpoint signalling is uncoupled from chromosomal position in mouse oocytes. *Development.* 139:1941–1946. http://dx.doi.org/10.1242/dev.078352

Hassold, T., and P. Hunt. 2001. To err (meiotically) is human: The genesis of human aneuploidy. *Nat. Rev. Genet.* 2:280–291. http://dx.doi.org/10.1038/35066065

Hodges, C.A., and P.A. Hunt. 2002. Simultaneous analysis of chromosomes and chromosome-associated proteins in mammalian oocytes and embryos. *Chromosoma.* 111:165–169. http://dx.doi.org/10.1007/s00412-002-0195-3

Holt, J.E., and K.T. Jones. 2009. Control of homologous chromosome division in the mammalian oocyte. *Mol. Hum. Reprod.* 15:139–147. http://dx.doi.org/10.1093/molehr/gap007

Homer, H.A., A. McDougall, M. Levasseur, K. Yallop, A.P. Murdoch, and M. Herbert. 2005. Mad2 prevents aneuploidy and premature proteolysis of cyclin B and securin during meiosis I in mouse oocytes. *Genes Dev.* 19:202–207. http://dx.doi.org/10.1101/gad.328105

Howe, J.A., M. Howell, T. Hunt, and J.W. Newport. 1995. Identification of a developmental timer regulating the stability of embryonic cyclin A and a new somatic A-type cyclin at gastrulation. *Genes Dev.* 9:1164–1176. http://dx.doi.org/10.1101/gad.9.10.1164

Kabeche, L., and D.A. Compton. 2013. Cyclin A regulates kinetochore microtubules to promote faithful chromosome segregation. *Nature.* 502:110–113. http://dx.doi.org/10.1038/nature12507

Kalaszczynska, I., Y. Geng, T. Iino, S. Mizuno, Y. Choi, I. Kondratiuk, D.P. Silver, D.J. Wolgemuth, K. Akashi, and P. Sicinski. 2009. Cyclin A is redundant in fibroblasts but essential in hematopoietic and embryonic stem cells. *Cell.* 138:352–365. http://dx.doi.org/10.1016/j.cell.2009.04.062

Kanakkanthara, A., K.B. Jeganathan, J.F. Limzerwala, D.J. Baker, M. Hamada, H.J. Nam, W.H. van Deursen, N. Hamada, R.M. Naylor, N.A. Becker, et al. 2016. Cyclin A2 is an RNA binding protein that controls Mre11 mRNA translation. *Science.* 353:1549–1552. http://dx.doi.org/10.1126/science.aaf7463

Kok, F.O., M. Shin, C.W. Ni, A. Gupta, A.S. Grosse, A. van Impel, B.C. Kirchmaier, J. Peterson-Maduro, G. Kourkoulis, I. Male, et al. 2015. Reverse genetic screening reveals poor correlation between morpholino-induced and mutant phenotypes in zebrafish. *Dev. Cell.* 32:97–108. http://dx.doi.org/10.1016/j.devcel.2014.11.018

Kouznetsova, A., A. Hernández-Hernández, and C. Höög. 2014. Merotelic attachments allow alignment and stabilization of chromatids in meiosis II oocytes. *Nat. Commun.* 5:4409. http://dx.doi.org/10.1038/ncomms5409

Kreutzer, M.A., J.P. Richards, M.N. De Silva-Udawatta, J.J. Temenak, J.A. Knoblich, C.F. Lehner, and K.L. Bennett. 1995. *Caenorhabditis elegans* cyclin A- and B-type genes: A cyclin A multigene family, an ancestral cyclin B3 and differential germline expression. *J. Cell Sci.* 108:2415–2424.

Kudo, N.R., K. Wassmann, M. Anger, M. Schuh, K.G. Wirth, H. Xu, W. Helmhart, H. Kudo, M. McKay, B. Maro, et al. 2006. Resolution of chiasmata in oocytes requires separase-mediated proteolysis. *Cell.* 126:135–146. http://dx.doi.org/10.1016/j.cell.2006.05.033

Lan, Z.J., X. Xu, and A.J. Cooney. 2004. Differential oocyte-specific expression of Cre recombinase activity in *GDF-9-iCre*, *Zp3cre*, and *Msx2Cre* transgenic mice. *Biol. Reprod.* 71:1469–1474. http://dx.doi.org/10.1095/biolreprod.104.031757

Lefebvre, C., M.E. Terret, A. Djiane, P. Rassinier, B. Maro, and M.H. Verlhac. 2002. Meiotic spindle stability depends on MAPK-interacting and spindle-stabilizing protein (MISS), a new MAPK substrate. *J. Cell Biol.* 157:603–613. http://dx.doi.org/10.1083/jcb.200202052

Lewandoski, M., K.M. Wassarman, and G.R. Martin. 1997. *Zp3-cre*, a transgenic mouse line for the activation or inactivation of *loxP*-flanked target genes specifically in the female germ line. *Curr. Biol.* 7:148–151. http://dx.doi.org/10.1016/S0960-9822(06)00059-5

Liu, D., M.M. Matzuk, W.K. Sung, Q. Guo, P. Wang, and D.J. Wolgemuth. 1998. Cyclin A1 is required for meiosis in the male mouse. *Nat. Genet.* 20:377–380. http://dx.doi.org/10.1038/3855

Madgwick, S., D.V. Hansen, M. Levasseur, P.K. Jackson, and K.T. Jones. 2006. Mouse Emi2 is required to enter meiosis II by reestablishing cyclin B1 during interkinesis. *J. Cell Biol.* 174:791–801. http://dx.doi.org/10.1083/jcb.200604140

Marangos, P., and J. Carroll. 2004. Fertilization and $InsP_3$-induced Ca^{2+} release stimulate a persistent increase in the rate of degradation of cyclin B1 specifically in mature mouse oocytes. *Dev. Biol.* 272:26–38. http://dx.doi.org/10.1016/j.ydbio.2004.04.012

McCleland, M.L., J.A. Farrell, and P.H. O'Farrell. 2009. Influence of cyclin type and dose on mitotic entry and progression in the early *Drosophila* embryo. *J. Cell Biol.* 184:639–646. http://dx.doi.org/10.1083/jcb.200810012

Minshull, J., R. Golsteyn, C.S. Hill, and T. Hunt. 1990. The A- and B-type cyclin associated cdc2 kinases in *Xenopus* turn on and off at different times in the cell cycle. *EMBO J.* 9:2865–2875.

Murphy, M., M.G. Stinnakre, C. Senamaud-Beaufort, N.J. Winston, C. Sweeney, M. Kubelka, M. Carrington, C. Bréchot, and J. Sobczak-Thépot. 1997. Delayed early embryonic lethality following disruption of the murine cyclin A2 gene. *Nat. Genet.* 15:83–86. http://dx.doi.org/10.1038/ng0197-83

Nasmyth, K. 2002. Segregating sister genomes: The molecular biology of chromosome separation. *Science.* 297:559–565. http://dx.doi.org/10.1126/science.1074757

Perry, A.C., and M.H. Verlhac. 2008. Second meiotic arrest and exit in frogs and mice. *EMBO Rep.* 9:246–251. http://dx.doi.org/10.1038/embor.2008.22

Persson, J.L., Q. Zhang, X.Y. Wang, S.E. Ravnik, S. Muhlrad, and D.J. Wolgemuth. 2005. Distinct roles for the mammalian A-type cyclins during oogenesis. *Reproduction.* 130:411–422. http://dx.doi.org/10.1530/rep.1.00719

Pesin, J.A., and T.L. Orr-Weaver. 2007. Developmental role and regulation of cortex, a meiosis-specific anaphase-promoting complex/cyclosome activator. *PLoS Genet.* 3:e202. http://dx.doi.org/10.1371/journal.pgen.0030202

Peters, J.M. 2006. The anaphase promoting complex/cyclosome: A machine designed to destroy. *Nat. Rev. Mol. Cell Biol.* 7:644–656. http://dx.doi.org/10.1038/nrm1988

Pines, J., and T. Hunter. 1990. Human cyclin A is adenovirus E1A-associated protein p60 and behaves differently from cyclin B. *Nature.* 346:760–763. http://dx.doi.org/10.1038/346760a0

Pines, J., and T. Hunter. 1991. Human cyclins A and B1 are differentially located in the cell and undergo cell cycle-dependent nuclear transport. *J. Cell Biol.* 115:1–17. http://dx.doi.org/10.1083/jcb.115.1.1

Rattani, A., P.K. Vinod, J. Godwin, K. Tachibana-Konwalski, M. Wolna, M. Malumbres, B. Novák, and K. Nasmyth. 2014. Dependency of the spindle assembly checkpoint on Cdk1 renders the anaphase transition irreversible. *Curr. Biol.* 24:630–637. http://dx.doi.org/10.1016/j.cub.2014.01.033

Rauh, N.R., A. Schmidt, J. Bormann, E.A. Nigg, and T.U. Mayer. 2005. Calcium triggers exit from meiosis II by targeting the APC/C inhibitor XErp1 for degradation. *Nature.* 437:1048–1052. http://dx.doi.org/10.1038/nature04093

Rossi, A., Z. Kontarakis, C. Gerri, H. Nolte, S. Hölper, M. Krüger, and D.Y. Stainier. 2015. Genetic compensation induced by deleterious mutations but not gene knockdowns. *Nature.* 524:230–233. http://dx.doi.org/10.1038/nature14580

Sako, K., K. Suzuki, M. Isoda, S. Yoshikai, C. Senoo, N. Nakajo, M. Ohe, and N. Sagata. 2014. Emi2 mediates meiotic MII arrest by competitively inhibiting the binding of Ube2S to the APC/C. *Nat. Commun.* 5:3667. http://dx.doi.org/10.1038/ncomms4667

Shoji, S., N. Yoshida, M. Amanai, M. Ohgishi, T. Fukui, S. Fujimoto, Y. Nakano, E. Kajikawa, and A.C. Perry. 2006. Mammalian Emi2 mediates cytostatic arrest and transduces the signal for meiotic exit via Cdc20. *EMBO J.* 25:834–845. http://dx.doi.org/10.1038/sj.emboj.7600953

Shomper, M., C. Lappa, and G. FitzHarris. 2014. Kinetochore microtubule establishment is defective in oocytes from aged mice. *Cell Cycle.* 13:1171–1179. http://dx.doi.org/10.4161/cc.28046

Sigrist, S., H. Jacobs, R. Stratmann, and C.F. Lehner. 1995. Exit from mitosis is regulated by *Drosophila* fizzy and the sequential destruction of cyclins A, B and B3. *EMBO J.* 14:4827–4838.

Sluder, G., E.A. Thompson, F.J. Miller, J. Hayes, and C.L. Rieder. 1997. The checkpoint control for anaphase onset does not monitor excess numbers of spindle poles or bipolar spindle symmetry. *J. Cell Sci.* 110:421–429.

Smart, N., and P.R. Riley. 2013. Thymosin β4 in vascular development response to research commentary. *Circ. Res.* 112:e29–e30. http://dx.doi.org/10.1161/CIRCRESAHA.112.300555

Suzuki, T., E. Suzuki, N. Yoshida, A. Kubo, H. Li, E. Okuda, M. Amanai, and A.C. Perry. 2010. Mouse Emi2 as a distinctive regulatory hub in second meiotic metaphase. *Development.* 137:3281–3291. http://dx.doi.org/10.1242/dev.052480

Sweeney, C., M. Murphy, M. Kubelka, S.E. Ravnik, C.F. Hawkins, D.J. Wolgemuth, and M. Carrington. 1996. A distinct cyclin A is expressed in germ cells in the mouse. *Development.* 122:53–64.

Swenson, K.I., K.M. Farrell, and J.V. Ruderman. 1986. The clam embryo protein cyclin A induces entry into M phase and the resumption of meiosis in *Xenopus* oocytes. *Cell.* 47:861–870. http://dx.doi.org/10.1016/0092-8674(86)90801-9

Terret, M.E., C. Lefebvre, A. Djiane, P. Rassinier, J. Moreau, B. Maro, and M.H. Verlhac. 2003. DOC1R: A MAP kinase substrate that control microtubule organization of metaphase II mouse oocytes. *Development.* 130:5169–5177. http://dx.doi.org/10.1242/dev.00731

Thompson, S.L., and D.A. Compton. 2011. Chromosome missegregation in human cells arises through specific types of kinetochore–microtubule attachment errors. *Proc. Natl. Acad. Sci. USA.* 108:17974–17978. http://dx.doi.org/10.1073/pnas.1109720108

Touati, S.A., D. Cladière, L.M. Lister, I. Leontiou, J.P. Chambon, A. Rattani, F. Böttger, O. Stemmann, K. Nasmyth, M. Herbert, and K. Wassmann. 2012. Cyclin A2 is required for sister chromatid segregation, but not separase control, in mouse oocyte meiosis. *Cell Reports.* 2:1077–1087. http://dx.doi.org/10.1016/j.celrep.2012.10.002

Uhlmann, F. 2003. Chromosome cohesion and separation: From men and molecules. *Curr. Biol.* 13:R104–R114. http://dx.doi.org/10.1016/S0960-9822(03)00039-3

Wakayama, Y., S. Fukuhara, K. Ando, M. Matsuda, and N. Mochizuki. 2015. Cdc42 mediates Bmp-induced sprouting angiogenesis through Fmnl3-driven assembly of endothelial filopodia in zebrafish. *Dev. Cell.* 32:109–122. http://dx.doi.org/10.1016/j.devcel.2014.11.024

Walker, D.H., and J.L. Maller. 1991. Role for cyclin A in the dependence of mitosis on completion of DNA replication. *Nature.* 354:314–317. http://dx.doi.org/10.1038/354314a0

Winston, N., F. Bourgain-Guglielmetti, M.A. Ciemerych, J.Z. Kubiak, C. Senamaud-Beaufort, M. Carrington, C. Bréchot, and J. Sobczak-Thépot. 2000. Early development of mouse embryos null mutant for the cyclin A2 gene occurs in the absence of maternally derived cyclin A2 gene products. *Dev. Biol.* 223:139–153. http://dx.doi.org/10.1006/dbio.2000.9721

Wolgemuth, D.J. 2011. Function of the A-type cyclins during gametogenesis and early embryogenesis. *Results Probl. Cell Differ.* 53:391–413. http://dx.doi.org/10.1007/978-3-642-19065-0_17

Wolthuis, R., L. Clay-Farrace, W. van Zon, M. Yekezare, L. Koop, J. Ogink, R. Medema, and J. Pines. 2008. Cdc20 and Cks direct the spindle checkpoint-independent destruction of cyclin A. *Mol. Cell.* 30:290–302. http://dx.doi.org/10.1016/j.molcel.2008.02.027

Yang, R., R. Morosetti, and H.P. Koeffler. 1997. Characterization of a second human cyclin A that is highly expressed in testis and in several leukemic cell lines. *Cancer Res.* 57:913–920.

Yoshida, S., M. Kaido, and T.S. Kitajima. 2015. Inherent instability of correct kinetochore-microtubule attachments during meiosis I in oocytes. *Dev. Cell.* 33:589–602. http://dx.doi.org/10.1016/j.devcel.2015.04.020

Zhai, Y., P.J. Kronebusch, and G.G. Borisy. 1995. Kinetochore microtubule dynamics and the metaphase-anaphase transition. *J. Cell Biol.* 131:721–734. http://dx.doi.org/10.1083/jcb.131.3.721